# Supporting Information

*Shuiting Luo [a], Mingyue Lv [a], Ye Tian [bc], Lin Jiang [a], Keying Shi *[a], and Li Li*[ab]*

[a] *Key Laboratory of Functional Inorganic Material Chemistry, Ministry of Education. School of Chemistry and Material Science, Heilongjiang University, Harbin, 150080, P. R. China.*

[b] *College of Modern Agriculture and Ecological Environment, Heilongjiang University, Harbin 150080, P. R. China*

[c] *Department of Mechanical Engineering, The University of Hong Kong, Pokfulam, Hong Kong Special Administrative Region*

***Corresponding author**

Tel.: +86 451 86604920; +86 451 86609141

Email: lili1993036@hlju.edu.cn, shikeying2008@163.com

# Table of contents

**Table. S1** Current performance of typical gas sensors based on bimetallic and trimetallic composites in literature reports.

| Samples | Application | Operation temperature | Response/concentration | References |
|---|---|---|---|---|
| NiAl-LDHs | $O_3$ gas sensor | RT | 1.84/700 ppb | [1] |
| $Zn_2Al$-LDHs | Ethanol gas sensor | 240 °C | 12.5/100 ppm | [2] |
| NiCo-LDHs | $NO_x$ gas sensor | RT | 70%/97 ppm | [3] |
| Pt/ZnAl-LDHs | $CH_4$ gas sensor | 450 °C | 5/500 ppm | [4] |
| HPTS/NiFe-LDHs | $CO_2$ gas sensor | RT | --/-- | [5] |
| Mg-Al-LDHs | $NO_x$ gas sensor | RT | 76%/100 ppm | [6] |
| PANI/ZnTi-LDHs | $NH_3$ gas sensor | RT | 20/50 ppm | [7] |
| CoAl-LDHs | $NO_x$ gas sensor | RT | 17.09/100 ppm | [8] |
| Ni-Cr-Al-LDHs | Ethanol gas sensor | RT | 8.24/1000ppm | [9] |
| | Acetone gas sensor | | 11.31/1000 ppm | |
| Ni-Fe-Al-LDHs | $NO_x$ gas sensor | RT | 82%/100 ppm | [10] |
| PS@Co-LDHs | Ethanol gas sensor | 200 °C | 2.48/4.3 ppm | [11] |
| | Dimethyl sulfide gas sensor | | 3/125ppm | |
| Co-LDHs | $NO_2$ gas sensor | RT | 23.7/100 ppm | This work |

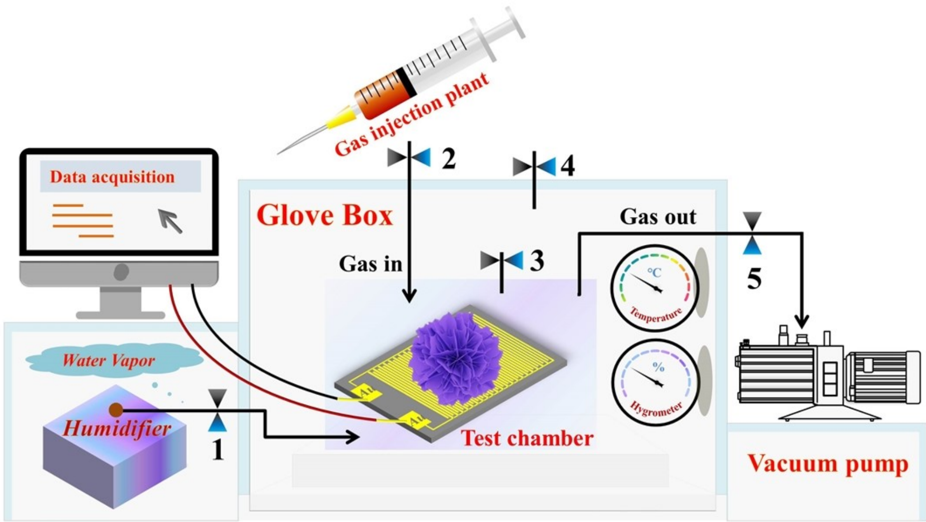


**Fig. S1** The diagram of the gas delivery system for the gas sensing process.

The steps are as follows:

First, the interdigitated gold electrode sensor is mounted in the test chamber, when the valves 3, 4, 5 remain open and the test chamber is flushed with air for at least 3 minutes to remove distractors from the test chamber and the homemade glove box. Then, valve 5 is closed, valve 1 is opened to inject steam into the test chamber and observe the tank hygrometer until the test chamber and glove box reach the target humidity, and then close valves 1, 3 and 4. Finally, open the valve 2 and inject a certain volume of $NO_2$ gas to record the resistance change. When the resistance is balanced, valves 5 and 4 are opened successively, and the vacuum pump is used to clean the chamber to restore the sensor resistance to its original state. The above is a full response recovery cycle. The first three phases were repeated, the $NO_2$ gas concentration was controlled with a micro-syringe, the $NO_2$ was injected into the test chamber to complete a second response recovery cycle, and then measure the recording resistance changes and so on.

**Fig. S2** The Tyndall effect of the CCM-2 colloidal solution.

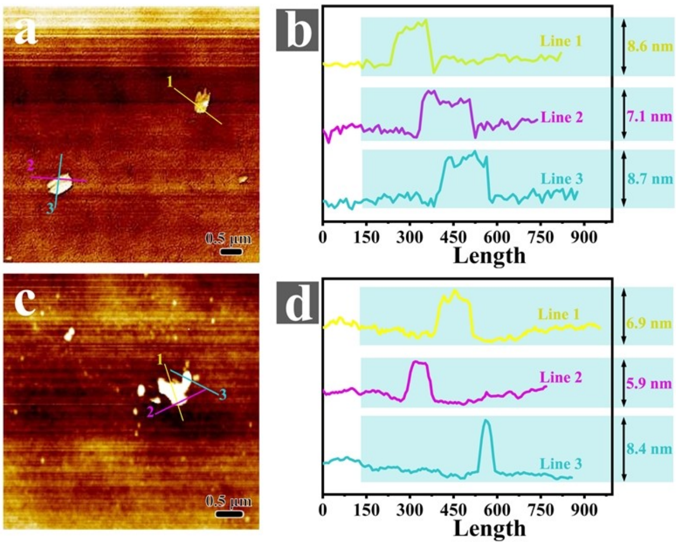


**Fig. S3** AFM images and height profiles of CCM-1 (a, b) andCCM-3 (c, d)

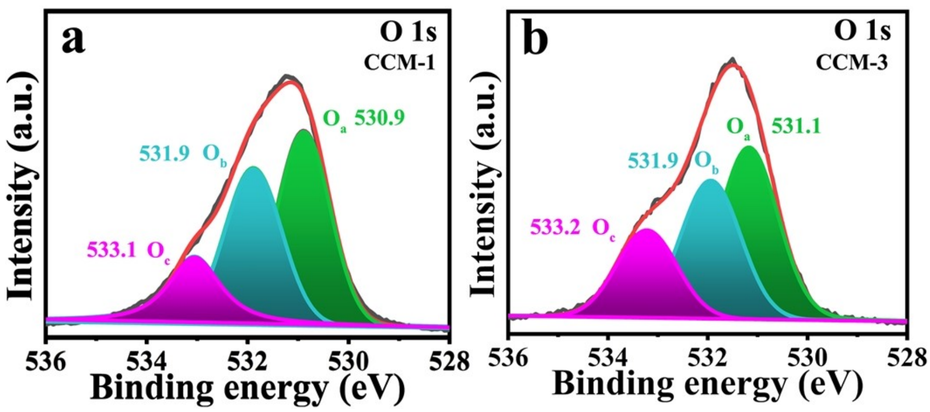


**Fig. S4** O 1s high-resolution XPS survey spectra of (a) CCM-1 and (b) CCM-3, respectively.

**Table. S2** O 1s peak position and peak area ratio (%) of the four samples

| Sample | CCM-1 | CCM-2 | CCM-3 | CCM-2+$NO_2$ |
|---|---|---|---|---|
| Peak | $O_a$, $O_b$, $O_c$ | $O_a$, $O_b$, $O_c$ | $O_a$, $O_b$, $O_c$ | $O_a$, $O_b$, $O_c$ |
| Peak position (eV) | 530.9, 531.9, 533.1 | 531.1, 532.2, 533.5 | 531.1, 531.9, 533.2 | 531.4, 532.1, 533.2 |
| Peak area ratio (%) | 43.90, 35.78, 20.32 | 41.73, 32.96, 25.31 | 42.72, 35.36, 21.92 | 32.00, 23.78, 44.22 |

*$O_a$: lattice oxygen; $O_b$: oxygen deficiency/vacancies structure; $O_c$: chemisorbed oxygen.

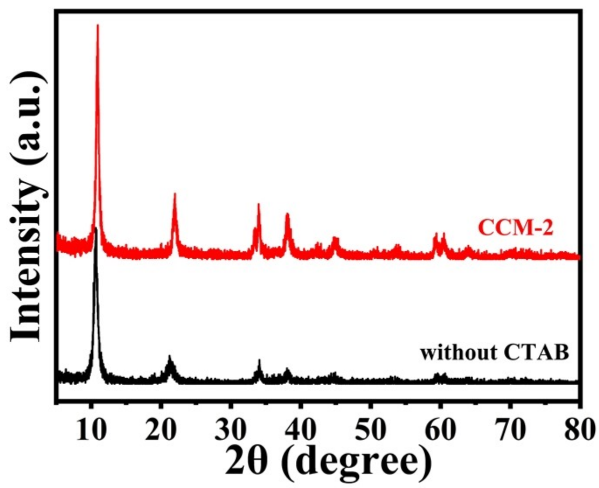


**Fig. S5** XRD patterns of the CCM-2 with and without CTAB.

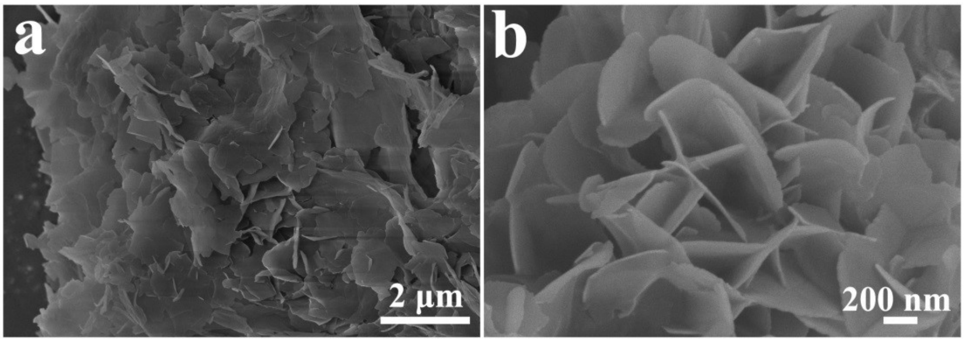


**Fig. S6** SEM images of CCM-2 (a) with and (b) without CTAB.

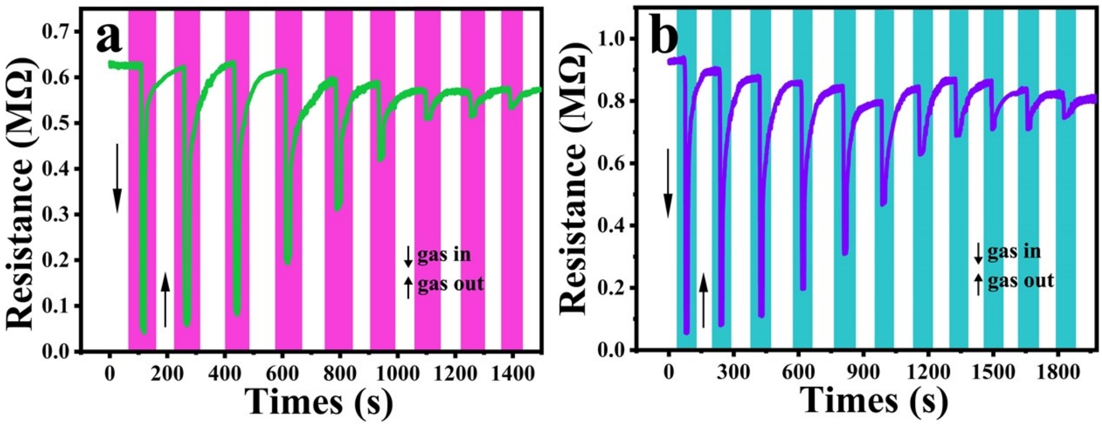


**Fig. S7** The dynamical response/recovery transient curves of (a) CCM-1 sensor to 100-0.3 ppm $NO_2$ and (b) CCM-3 sensor to 100-0.05 ppm $NO_2$.

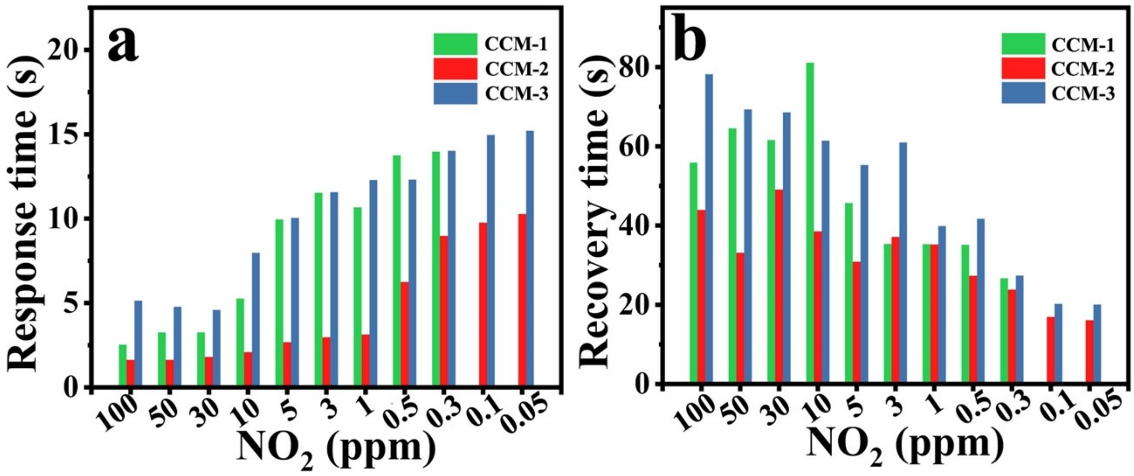


**Fig. S8** (a) Response time and (b) recovery time of the CCM-1, CCM-2 and CCM-3 sensor, respectively.

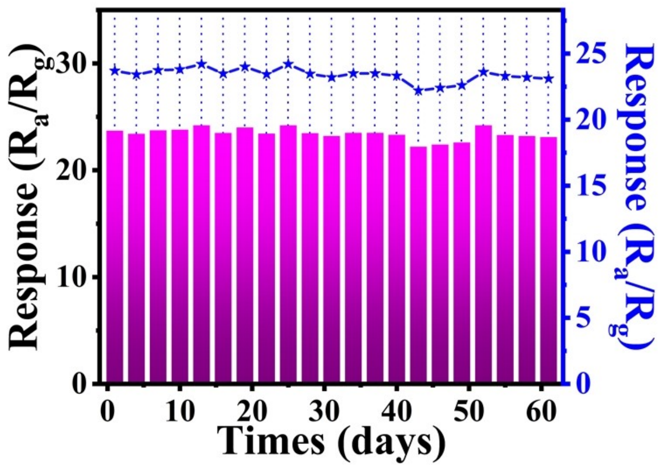


**Fig. S9** The stability of the CCM-2 sensor to 100 ppm $NO_2$ for 60 days at RT.

**Table. S3** The response, response time and recovery time of the three samples to different $NO_2$ concentrations at room temperature (RH: 26%)

| Sample | CCM-1 | | | CCM-2 | | | CCM-3 | | |
|---|---|---|---|---|---|---|---|---|---|
| $NO_2$ (ppm) | R | $T_s$ | $T_r$ | R | $T_s$ | $T_r$ | R | $T_s$ | $T_r$ |
| 100 | 15.39 | 2.53 | 55.87 | 23.70 | 1.63 | 43.93 | 16.81 | 5.14 | 78.21 |
| 50 | 10.91 | 3.26 | 64.53 | 14.19 | 1.63 | 33.13 | 11.17 | 4.78 | 69.32 |
| 30 | 7.84 | 3.26 | 61.59 | 10.90 | 1.81 | 49.06 | 7.83 | 4.59 | 68.56 |
| 10 | 3.20 | 5.26 | 81.12 | 6.49 | 2.09 | 38.54 | 4.36 | 7.97 | 61.42 |
| 5 | 1.92 | 9.95 | 45.68 | 3.27 | 2.68 | 30.87 | 2.56 | 10.05 | 55.29 |
| 3 | 1.41 | 11.53 | 35.36 | 2.30 | 2.97 | 37.12 | 1.71 | 11.57 | 60.98 |
| 1 | 1.12 | 10.67 | 35.29 | 1.64 | 3.13 | 35.21 | 1.34 | 12.29 | 39.86 |
| 0.5 | 1.09 | 13.75 | 35.15 | 1.41 | 6.24 | 27.33 | 1.26 | 12.31 | 41.72 |
| 0.3 | 1.05 | 13.97 | 26.67 | 1.33 | 8.98 | 23.83 | 1.21 | 14.02 | 27.37 |
| 0.1 | | | | 1.23 | 9.76 | 16.92 | 1.18 | 14.96 | 20.23 |
| 0.05 | | | | 1.19 | 10.27 | 16.09 | 1.08 | 15.21 | 20.08 |

*R: Response  $T_s$: Response time  $T_r$: Recovery time

## References


1 G. Kang, Z. Zhu, B.-H. Tang, C.-H. Wu and R.-J. Wu, *Sensors and Actuators B: Chemical*, 2017, **241**, 1203-1209.

2 M. Y. Guan, D. M. Xu, Y. F. Song and Y. Guo, *Sensors and Actuators B: Chemical*, 2013, **188**, 1148-1154.

3 Y. Ge, K. Kan, Y. Yang, L. Zhou, L. Jing, P. Shen, L. Li and K. Shi, *Journal of Materials Chemistry A*, 2014, **2**, 4961–4969.

4 S. Morandi, F. Prinetto, M. D. Martino, G. Ghiotti, O. Lorret, D. Tichit, C. Malagu, B. Vendemiati and M. C. Carotta, *Sens. Actuators, B*, 2006, **118**, 215-220.

5 H. Li, X. Su, C. Bai, Y. Xu, Z. Pei and S. Sun, Sens. Actuators, B, 2016, **225**, 109-114.

6 H. Sun, Z. Chu, D. Hong, G. Zhang, Y. Xie, L. Li and K. Shi, *Journal of Alloys and Compounds*, 2016, **658**, 561-568.

7 Q. Y, W. L and W. X, *Organic Electronics*, 2019, **66**, 102-9.

8 D. Wang, Z. Liu, Y. Hong, C. Lin, Q. Pan, L. Li and K. Shi, *RSC Advances*, 2020, **10**, 34466-34473.

9 S. O. Gheibi, A. Fallah Shojaei, A. Khorshidi and S. M. Hosseini-Golgoo, *Applied Physics A*, 2021, **127**, 614

10 D. Hong, J. Zhang, A. U. Rehman, L. Gong, J. Zhou, K. Kan, L. Li and K. Shi, *RSC Advances*, 2016, **6**, 103192-103198.

11 Y. Li, F. Zhou, L. Gao and G. Duan, *Sensors and Actuators B: Chemical*, 2018, **261**, 553-565.